http://dx.doi.org/10.5012/bkcs.2014.35.5.1422

Study of the Valence and Rydberg States of a Lithium Dimer by the Multi-reference Configuration-interaction Method

Chun-Woo Lee

Department of Chemistry, Ajou University, Woncheon-Dong, Yeongtong-Gu, Suwon 443-749, Korea
E-mail: clee@ajou.ac.kr
Received December 30, 2013, Accepted January 21, 2014

Convergent all-electron multi-reference configuration-interaction (MRCI) calculations are performed for a lithium dimer with Kaufmann's Rydberg basis functions. A comparison of the results of these calculations with those of the effective core potential/core polarization potential (ECP/CPP) method and experimental data reveals the deficiency of the all-electron *ab initio* method. The deficiency is related to the mere 51.9% attainment of electron correlation for the ground state. The percent attainment of electron correlation for the first excited state is slightly better than that for the ground state, preventing us from obtaining better agreements with experimental data by means of increasing the size of basis sets. The Kaufmann basis functions are then used with the ECP/CPP method to obtain the accurate convergent potential energy curves for the $^1\Pi_u$ states correlated to Li(2p) + Li(2p) and Li(2s) + Li(n = 2, 3, 4). Quantum defect curves (QDCs) calculated for both the X $^2\Sigma_g$ and 1 $^2\Pi_u$ states of the Li_2^+ ion and the Lu-Fano plot reveal a strong series-series interaction between the two 2snpπ and 2pnpπ Rydberg series. The QDCs are then used to resolve assignment problems in the literature. The reassignments, performed by Jedrzejewski-Szemek *et al.*, of the dissociation product of the D $^1\Pi_u$ state from (2s+3d) to (2s+3p) and that of the 6 $^1\Pi_u$ from (2s+4d) to (2s+4p) are found to be incorrect. It may be more natural to assign their 2snpπ Rydberg series as a 2sndπ series. The state, assigned as 5p $^1\Pi_u$ by Ross *et al.* and 4d $^1\Pi$ by Jedrzejewski-Szemek *et al.*, is assigned as the 7 $^1\Pi_u$ state, correlated to the Li(2s) + Li(4f) limit.

Key Words : Lithium dimer, Excited rydberg states, Multi-reference CI

Introduction

The modern theory of electronic structure is believed to be sufficient to calculate the potential energy surfaces of excited states, including Rydberg states, with chemical accuracy. Among the various methods designed to obtain the PESs of excited states, the multi-reference configuration-interaction (MRCI) method[1] is known to yield reliable values in most of cases. To obtain the PESs for the Rydberg states, the Rydberg basis functions[2] need to be included in the calculation in addition to the valence basis sets. Kaufmann's Rydberg basis functions were designed for this purpose.[3] Recently, we employed Kaufmann's Rydberg basis functions with the MRCI method to reproduce the potential energy curves (PECs) of HeH.[4] The advantages of using two different methods of locating Rydberg orbitals, either on the atomic nucleus or at the charge center of molecules, were exploited by limiting their application to different ranges of R. Using this method, the difference between the experimental binding energies of the lower Rydberg states obtained by Ketterle[5,6] and the *ab initio* results obtained by van Hemert and Peyerimhoff[7] was reduced from a few hundreds of wavenumbers to a few tens of wavenumbers. The substantial improvement in the accuracy allowed us to obtain the quantum defect curves of HeH, characterized by the correct behavior. We obtained several Rydberg series with more than one member, such as the ns (n = 2, 3, and 4), npσ (n = 3, 4), npπ (n = 2, 3, and 4), and ndπ (n = 3, 4) series. We now aim to apply this method to study the valence and Rydberg states of a lithium dimer.

The lithium dimer has drawn enormous attention from experimentalists and theoreticians. Its excited states can be easily accessed experimentally by using single- and two-photon visible dye lasers. It is the smallest bound homonuclear molecule beyond H_2 and may serve as a prototype for testing theoretical methods. The first *ab initio* calculations of Li_2 were performed by Konowalow *et al.*[8] Currently, all-electron *ab initio* calculations are rarely used[9-11] for this molecule, and most theoretical calculations are performed using the effective core potential (ECP) method.[12,13] The inclusion of the core polarization in this method is important because Li_2 has a highly polarizable Li_2^+ core. The core polarization potential (CPP), developed by Schmidt-Mink *et al.* and Fuentealba *et al.*,[12,14] is widely used now. Jasik and Sienkiewicz's work[13] using the ECP/CPP method is known to be the most accurate study on this molecule. Still, their calculation was limited to 25 states, while experiments have been performed for more excited states. There are several issues that cannot be answered definitively from spectroscopic observation alone without further *ab initio* calculations.[15]

Because there is no report describing why the theoretical calculations are dominated by the ECP/CPP methods for this molecule, we performed all-electron *ab initio* calculations augmented with the Kaufmann basis functions and compared the results with those of the ECP/CPP calculations and experimental data, and discussed the deficiencies of the all-

electron *ab initio* method. We then applied the Kaufmann basis method to the ECP/CPP method in order to obtain the convergent PECs. We then applied these PECs to the controversial assignment problems in the experimental data of the $^1\Pi_u$ states.

The MRCI method that is a part of the MOLPRO package[16] was used in the present study for the calculation of PECs. This method combines the multi-configuration self-consistent field (MCSCF) method of Werner, Meyer and Knowles and the internally contracted self-consistent electron pair theory for the MRCI method.[1]

All-electron *ab initio* Calculations

The MRCI method always yields reliable potential energy surfaces of the excited states of molecules. Any failure to obtain the correct PES is most presumably due to deficiencies either in the basis sets or in the choices of the active space and not in the MRCI method. For the calculation of the excited states, Dunning's correlation consistent basis set,[17] aug-cc-pVXZ (AVXZ) with X = T, Q, 5, and 6, is a well-designed set and yields excellent results for the energy calculations of the valence states. For the Rydberg states, the AVXZ basis set is not enough, and Rydberg basis functions need to be added. Usually, home-made Rydberg basis functions are added. In our previous reports, we used the universal Rydberg basis functions devised by Kaufmann.[3] There are two ways of incorporating Rydberg basis functions. One is to locate them on each nucleus, while the other is to locate them at the charge center of a molecule. Rydberg functions used in the former way are known as atomic Rydberg functions, and the ones used in the latter way are known as central Rydberg functions.[18]

Although complete active space (CAS) has many advantages,[19] incomplete active spaces are used for various reasons in the MCSCF method, which is performed prior to the MRCI calculations. Molecular orbitals that comprise active spaces are described by the irreducible representations of the symmetry group to which the molecules belong. The highest available symmetry group implemented in the MOLPRO package[16] for homonuclear diatomic molecules is the D_{2h} group, with eight irreducible representations: a_g, b_{3u}, b_{2u}, b_{1g}, b_{1u}, b_{2g}, b_{3g}, and a_u. For the states correlated to the dissociation products Li(2s) + Li(n = 2, 3, 4) and Li(2p) + Li(2p), only the Σ, Π, Δ, and Φ symmetries appear as shown in Table 1. We performed two kinds of state-averaging MRCI calculations. One is for the Σ and Δ symmetries, and the other is for the Π and Φ symmetries. For the excited state calculations belonging to the Σ and Δ symmetries up to n = 3, the CAS is given by ($7a_g$, $3b_{3u}$, $3b_{2u}$, $1b_{1g}$, 7b1u, $3b_{2g}$, $3b_{2u}$, $1a_u$). With this CAS, we can obtain 25 PECs (17 Σ and Δ and 8 Π), obtained in Ref [13], which is the best calculation available in the literature. Because more experimental PECs are obtained, larger active spaces are needed to obtain the corresponding theoretical PECs. The active space ($9a_g$, $3b_{3u}$, $3b_{2u}$, $1b_{1g}$, $9b_{1u}$, $3b_{2g}$, $3b_{2u}$, $1a_u$) is used to obtain up to twenty-two Σ and Δ states, and the active space ($5a_g$, $5b_{3u}$, $5b_{2u}$, $1b_{1g}$, $5b_{1u}$, $5b_{2g}$, $5b_{2u}$, $1a_u$) is used for twenty Π and Φ states. Figures 1 and 2 show the PECs obtained.

Comparison of the Spectroscopic Constants Obtained by Various Methods. The quality of the theoretically calculated PECs can be tested either by directly comparing them with the experimentally determined PECs or by indirectly comparing the spectroscopic constants calculated

Table 1. Molecular terms of a lithium dimer. Asymptotic energies are experimental values taken from NIST atomic spectra database (www.nist.gov). Numbers inside the parenthesis in the column of states denote another commonly used designations of states

Dissociation products	Asymptotic energy (cm^{-1})	States
$1s^22s\ ^2S_g + 1s^22s\ S_g$	0	X $^1\Sigma_g^+$, a $^3\Sigma_u^+$
$1s^22s\ ^2S_g + 1s^22p\ ^2P_u$	14903.89	2 $^1\Sigma_g^+$, A(1) $^1\Sigma_u^+$, 1 $^3\Sigma_g^+$, 2 $^3\Sigma_u^+$ G(1) $^1\Pi_g$, B(1) $^1\Pi_u$, 1 $^3\Pi_g$, b(1) $^3\Pi_u$
$1s^22s\ ^2S_g + 1s^23s\ ^2S_g$	27206.12	E(3) $^1\Sigma_g^+$, 2 $^1\Sigma_u^+$, 2 $^3\Sigma_g^+$, 3 $^3\Sigma_u^+$
$1s^22p^2P_u + 1s^22p\ ^2P_u$	29807.87	F(4) $^1\Sigma_g^+$, 5 $^1\Sigma_g^+$, 1 $^3\Sigma_g^-$, 4 $^3\Sigma_u^+$, 5 $^3\Sigma_u^+$, 1 $^1\Sigma_u^-$ 2 $^1\Pi_g$, 2 $^3\Pi_g$, C(2) $^1\Pi_u$, 2 $^3\Pi_u$, 1 $^1\Delta_g$, 1 $^3\Delta_u$
$1s^22s\ ^2S_g + 1s^23p\ ^2P_u$	30925.38	6 $^1\Sigma_g^+$, 3 $^1\Sigma_u^+$, 3 $^3\Sigma_g^+$, 6 $^3\Sigma_u^+$ 3 $^1\Pi_g$, 3 $^3\Pi_g$, D(3) $^1\Pi_u$, 3 $^3\Pi_u$
$1s^22s\ ^2S_g + 1s^23d\ ^2D_g$	31283.10	7 $^1\Sigma_g^+$, 4 $^1\Sigma_u^+$, 4 $^3\Sigma_g^+$, 7 $^3\Sigma_u^+$ 2 $^1\Delta_g$, 1 $^1\Delta_u$, 1 $^3\Delta_g$, 2 $^3\Delta_u$ 4 $^1\Pi_g$, 4 $^1\Pi_u$, 4 $^3\Pi_g$, 4 $^3\Pi_u$
$1s^22s\ ^2S_g + 1s^24s\ ^2S_g$	35012.06	8 $^1\Sigma_g^+$, 5 $^1\Sigma_u^+$, 5 $^3\Sigma_g^+$, 8 $^3\Sigma_u^+$
$1s^22s\ ^2S_g + 1s^24p\ ^2P_u$	36469.55	9 $^1\Sigma_g^+$, 6 $^1\Sigma_u^+$, 6 $^3\Sigma_g^+$, 9 $^3\Sigma_u^+$ 5 $^1\Pi_g$, 5 $^3\Pi_g$, 5 $^1\Pi_u$, 5 $^3\Pi_u$
$1s^22s\ ^2S_g + 1s^24d\ ^2D_g$	36623.4	10 $^1\Sigma_g^+$, 7 $^1\Sigma_u^+$, 7 $^3\Sigma_g^+$, 10 $^3\Sigma_u^+$, 3 $^1\Delta_g$, 2 $^1\Delta_u$, 2 $^3\Delta_g$, 3 $^3\Delta_u$ 6 $^1\Pi_g$, 6 $^1\Pi_u$, 6 $^3\Pi_g$, 6 $^3\Pi_u$
$1s^22s\ ^2S_g + 1s^24f\ ^2F_u$	36630.2	11 $^1\Sigma_g^+$, 8 $^1\Sigma_u^+$, 8 $^3\Sigma_g^+$, 11 $^3\Sigma_u^+$ 4 $^1\Delta_g$, 3 $^1\Delta_u$, 3 $^3\Delta_g$, 4 $^3\Delta_u$ 7 $^1\Pi_g$, 7 $^1\Pi_u$, 7 $^3\Pi_g$, 7 $^3\Pi_u$, 1 $^1\Phi_g$, 1 $^1\Phi_u$, 1 $^3\Phi_g$, 1 $^3\Phi_t$

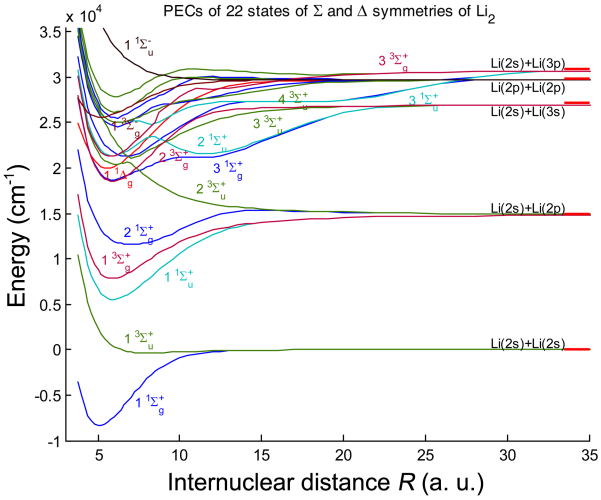

Figure 1. PECs of the Σ and Δ symmetries of a lithium dimer obtained by the all-electron *ab initio* MRCI method. Different symmetries are distinguished on the basis of color.

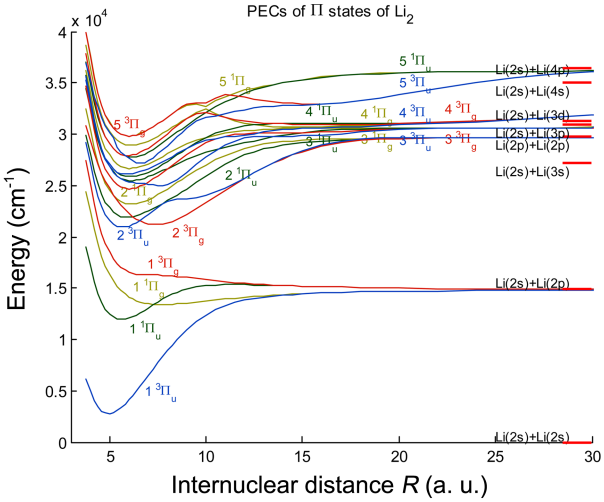

Figure 2. PECs of the Π and Φ symmetries of a lithium dimer obtained by the all-electron *ab initio* MRCI method. Different symmetries are distinguished on the basis of color.

from the theoretical PECs with the observed ones. We first consider the comparison of the spectroscopic constants.

In Table 2, the spectroscopic constants obtained from the PECs of this work are compared with the values obtained by Jasik and Sienkiewicz[13] using the ECP/CPP method and with the experimental values. (The references for the experimental data are not provided in the table. Please refer to Ref. [13]). In Figure 3, the errors in the calculations of R_e, D_e, and T_e by the all-electron *ab initio* and ECP/CPP methods are compared with the experimental data. It is observed that the ECP/CPP method produces better results than the all-electron *ab initio* calculations except for the three states 1 $^1\Sigma_u^+$, 1 $^3\Sigma_u^+$, and 1 $^3\Sigma_g^+$ for D_e. Considering that the orbital exponents of the matching basis set for the ECP/CPP method are the only adjusted parameters to yield the experimental values of the energy of the states in the dissociation limit, the impressive achievement of the ECP/CPP method indicates that the core electron correlation and polarization effects are properly accounted for in the effective core potential and core polarization potential. The equilibrium bond distances, R_e, calculated by the all-electron *ab initio* calculations are longer than those of the experimental values. The differences are mostly less than 0.04 Å except for 2 $^1\Sigma_u^+$ (outer well) and 2 $^3\Pi_g$. The differences for the latter are as large as 0.1 Å, while the equilibrium distances obtained by the ECP/CPP method agree much better with the experimental data. The all-electron *ab initio* calculations produce good results for the calculation of D_e but yield poor results for T_e, differing from the experimental values by 200-500 cm^{-1}. Although the errors in T_e are within the acceptable range for this kind of calculation, the errors are still ten times larger than our recently obtained results for HeH.[4] Apart from the large magnitude of the errors, the sign of the errors in T_e is a problematic aspect. Errors with this sign cannot be diminished by increasing the size of the Rydberg (or diffuse) basis set. The values of T_e are already lower than the experimental values and the additional Rydberg basis functions lower the energy of a state more as the state is more highly excited. This kind of problem was previously observed[4] but was ignored because of the small size of the negative values of errors. However, the size of the errors here is too large to be ignored. This problem will be discussed in the next section.

The comparison of the PECs of this work are made with those reported in Ref. [13] and the experimental PECs obtained by the Rydberg-Klein-Rees method,[20] the inverted perturbation approach method[21] and the direct potential fit.[22] More than thirty PECs are determined experimentally. The comparison is limited to the cases where other all-electron *ab initio* results are available. The ECP/CPP results are also compared together if they are available. Since the comparison only confirms the previous results obtained from the spectroscopic constants, it is relegated into the Supplementary material. Refer to the Supplementary material for the comparison graphs.

Effective Core Potential/Core Polarization Potential Calculations. The previous section shows that the all-electron *ab initio* method yields results showing rather good agreements with the experimental data. But, the agreements are not as good as those obtained from the ECP/CPP method. The equilibrium distances are overestimated. The values of T_e are lower than the experimental values by 200-500 cm^{-1}, and thus cannot be improved by increasing the size of Rydberg basis set. Overall, the all-electron *ab initio* MRCI method currently available is insufficient for the lithium dimer. Efforts to further improve the accuracy of this method have failed with the current version of MOLPRO. Table 3 provides a clue to this failure. According to the table, only 52% of the electron correlation energy is attained for the ground state of Li by the MRCI method with the largest correlated basis set (AV5Z for Li), while 99.4% of the electron correlation energy is attained by the same method (with the AV6Z basis set) for He.

Table 3 also shows that the percent electron correlation energy attained for the Li ground state by the MRCI method

Table 2. Comparison of the spectroscopic parameters R_e (Å), D_e, and T_e (cm^{-1}) of a lithium dimer obtained by ECP/CPP method, from the all-electron *ab initio* PECs of this work with those of experimental data. The values of experimental data are taken from Ref. [13]

State	ECP/CPP[13]			All-electron (this work)			Exp.		
	R_e	D_e	T_e	R_e	D_e	T_e	R_e	D_e	T_e
$1\ ^1\Sigma_g^+$	2.658	8613	0	2.700	8355	0	2.673	8516.78	0
$2\ ^1\Sigma_g^+$	3.655	3285	20171	3.719	3247	19896	3.651	3319	20101
$3\ ^1\Sigma_g^+$	3.076	8328	27414	3.115	8216	27005	3.086	8312.8	27410
$4\ ^1\Sigma_g^+$ inner well	3.545	8403	29960	3.599	8447	29548	3.548	8349.3	29975
$4\ ^1\Sigma_g^+$ outer well	9.1	2173	36190	9.069	2374	35621			
$1\ ^1\Sigma_u^+$	3.092	9486	13962	3.141	9322	13813	3.108	9352.5	14068
$2\ ^1\Sigma_u^+$ inner well	3.081	5674	30067	3.125	5568	29653	3.096		30101.407
$2\ ^1\Sigma_u^+$ outer well	6.072	5413	30329	6.135	55367	29853	36.037		30400.137
$3\ ^1\Sigma_u^+$ inner well	4.369	5854	33618	3.288	5663	33300			
$3\ ^1\Sigma_u^+$ outer well	9.275	3232	36240	4.384	3336	33091			
$1\ ^3\Sigma_u^+$	4.134	344	8196	4.212	337	7945	4.171	333	8183.8
$2\ ^3\Sigma_u^+$	3.182	-5669	29124	3.221	-5564	28706			
$3\ ^3\Sigma_u^+$	3.658	5898	29844	3.722	5854	29367			
$4\ ^3\Sigma_u^+$	3.351	4172	34191	3.285	4684	33311			
$5\ ^3\Sigma_u^+$ inner well	3.149	3275	35088	3.151	4043	33952			
$5\ ^3\Sigma_u^+$ outer well	5.626	226	38137	3.182	3553	34442			
$1\ ^3\Sigma_g^+$	3.053	7184	16264	3.106	7013	16122	3.068	7091.5	16328.8
$2\ ^3\Sigma_g^+$	3.073	8451	27291	3.114	8360	26861			
$1\ ^1\Pi_g$	4.048	1432	22018	4.082	1437	21700	4.058	1422.5	21968
$2\ ^1\Pi_g$	3.191	6469	31894	3.237	6550	31446	3.201	6455	31868.4
$1\ ^1\Pi_u$	2.934	2939	20514	2.977	2915	20226	2.936	2984.5	20436
$2\ ^1\Pi_u$	3.077	7765	30598	3.119	7814	30182	3.074	7648.4	30549
$2\ ^3\Pi_g$	3.853	8511	29852	3.917	8542	29454	3.816	8484	29840.5
$1\ ^3\Pi_u$	2.577	12302	11148	2.621	12072	11065			
$2\ ^3\Pi_u$	2.968	8720	29643	3.010	8774	29222			
$2\ 1\Delta_g$	2.822	8811	29552	2.946	9702	28293		9579	

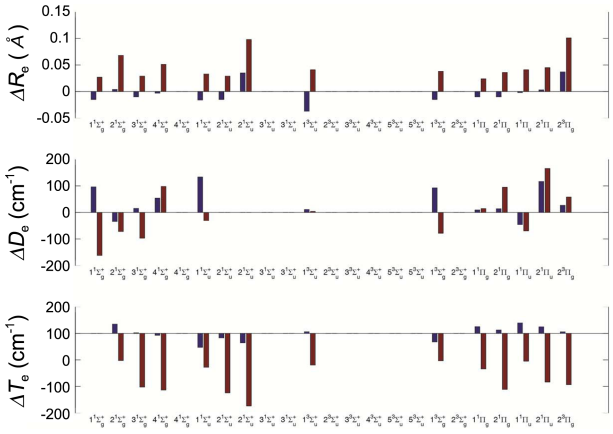

Figure 3. Errors in the calculations of R_e, D_e, and T_e by the ECP/CPP and all-electron *ab initio* methods compared to the experimental data. The first (blue) and second (red) bars for each state denote the errors in the ECP/CPP and all-electron *ab initio* methods, respectively.

Table 3. Percent electron correlation energies of the MRCI method in He and Li atoms. Hartree-Fock energies are obtained by the program developed by Fischer[49]

	Energy (a. u.)		
	He $1s^2\ ^1S$	He $1s2p\ ^3P$	
E_{HF}	−2.8616731	−2.1314371	
E_{MRCI} (AV6Z)	−2.9034553	−2.0857630	
E_{Exact}[50]	−2.9037244	−2.1331642	
% corr	99.4		
	Energy (a. u.)		ΔE (cm^{-1})
	Li $1s^22s\ ^2S$	Li $1s^22p\ ^2P$	
E_{HF}	−7.432727	−7.365070	14849
E_{MRCI} (AV5Z)	−7.456276	−7.388777	14814
E_{Exact}[51]	−7.478060	−7.410160	14902
% corr	51.9	52.6	
	Experimental value		14903

is smaller than that attained for the excited 2p ^{2}P state. In other words, the excited state is calculated better than the ground state. This may be due to the large dipole polarizability (theoretical value: 59 a. u.[23]) of the Li_2^+ ion core. The large polarizability of the ion core means that the electron correlation is larger in the ground state than in the excited state. This causes the previously described problem of smaller calculated excitation energy than the experimentally observed excitation energy.

The above result indicates that there is a limit to the accuracy we can achieve with all-electron *ab initio* calculations. In contrast to all-electron *ab initio* calculations, the current effective core potential method incorporated with the core polarization potential (ECP/CPP) yields results that more closely agree with experimental values. Moreover, the ECP/CPP method reduces the number of participating electrons and thus allows us to calculate higher states. This method is thus more appropriate for the study of Rydberg states. We used this method to study the Rydberg states of $^1\Pi_u$ symmetry, for which numerous experiments have been performed.[15,24-38] Several ambiguities are present in the interpretation of the experimental data for the states lying higher than the third member of this symmetry, and theoretical calculations are thus highly anticipated.[15] Two theoretical studies were conducted on these states but these are not published yet; one is presented in a Ph.D. thesis,[39] and another is presented as a poster,[40] available on the internet. Both studies are incomplete. The latter study is known to produce better results than the former. The present work may be considered as an extension of the latter study. The main extensions to the methods are the use of different active spaces in a different range of internuclear distances, and the use of several basis sets if they are needed in order to obtain the convergence of the results.

We used the ECP/CPP and the associated valence basis set, as obtained by the Stuttgart/Koen group,[14] known as ECP2SDF with the dipole polarizability α_D and the cutoff parameter δ, given by 0.1915 and 0.831 in a.u., respectively. The associated valence basis set known as CC-PV5Z, which is composed of 4s, 4p, 4d, 3f, and 2g functions, is only available by private communication with Stoll. Because this basis set is only good for atomic states up to $n = 2$ Li, Jasik and Sienkiewicz added three s, three p, and two d core functions and two s, two p, and two d diffuse orbitals. Let us call this set as the JS set. This set is composed of (9s, 9p, 8d, 3f, 2g) functions. With this basis set, errors in the energies of the 2s, 2p, 3s, and 3p atomic Li states compared with the experimental data are less than 8 cm^{-1}, as shown in Table 1 of Ref [13]. Note that the Li atom has only one electron in the ECP/CPP method, and the states can be labeled with the atomic orbital notation.

For a better representation of the 3d and $n = 4$ states, a larger basis set is required. Two larger basis sets have been used so far. One set, composed of (27s, 17p, 14d, 6f, 2g) functions, is developed by Gadea's group.[41] The other set, developed by Jasik and Sienkiewicz,[40] is an extension of the JS set to (12s, 12p, 12d, 10f, 2g) functions. For the calculation of the Π and Φ states, the newly added core functions are not necessary and can be omitted without affecting the results. With this consideration, the extended JS set is downsized to (10s, 10p, 10d, 5f, 2g) functions. In case of the set developed by the Gadea group (referred to hereafter as the GA set), errors in the energies of the Li atomic states are less than 6 cm^{-1} only up to the 5p orbital, while errors in the case of the extended JS set are less than 9 cm^{-1} up to the 4s orbital. For the 4p and 4d levels, the errors are 24 and 190 cm^{-1}, respectively. Although the GA set gives better results, its size is larger than that of the extended JS set. The set where the diffuse functions of the extended JS set are replaced by the corresponding functions of the GA set gives an error of less than 8 cm^{-1} up to the 5s level while keeping its size small. Let us call this combined set as the JSGA set (in order to get the JS, GA, and JSGA sets, please refer to the supplementary material). Although the JSGA set yields good results for the atomic energy levels, MRCI calculations with the set are numerically unstable in the chemical bonding region. The extended JS set is used in the bonding region instead. Therefore, two different basis sets are used at different ranges of internuclear distance R.

If the number of states in the state-averaged calculation is as large as twenty, the numerical stability is highly susceptible to the choice of active spaces. Numerical stability is acquired in the active space ($2a_g$, $7b_{3u}$, $7b_{2u}$, $2b_{1g}$, $1b_{1u}$, $4b_{2g}$, $4b_{2u}$, $1a_u$) at 4.6 $a_0 \le R \le 11$ a_0 for the extended JS set for the twenty state-averaged calculations composed of four, eight, four, and four states of $^1\Pi_g$, $^1\Pi_u$, $^3\Pi_g$, and $^3\Pi_u$ symmetries, respectively. The energies of these 20 states are not further lowered after adding the (3p, 4d, 5f, 3g) Kaufmann basis functions to the extended JS valence set (see the supplementary material for the used Kaufmann basis set). For the range of R smaller than 4.6 a_0, the calculation becomes unstable. It is stabilized with the Kaufmann set (3p, 4d, 5f, 2d) in the 4.0-4.4 a_0 range of R and with the Kaufmann (3f) function in the 3.2-3.8 a_0 range of R. The PECs obtained from these two calculations are combined to obtain the PECs at $R < 4.6$ a_0. These PECs connect smoothly to the PECs at $R \ge 4.6$ a_0 and are used for the calculation of the QDCs. Because convergence cannot be confirmed, caution should be taken in using the PECs at $R < 4.6$ a_0. The spectroscopic constants can be obtained without including this unguaranteed range of R.

Figure 4 shows the PECs of the lowest seven $^1\Pi_u$ states and one $^1\Phi_u$ state. Another $^1\Pi_u$ state, shown by the thick dashed line, is partially obtained. The reference energy is taken as the Li(2s) + Li(2s) dissociation limit. Several comments are in order for Figure 4. Firstly, the $^1\Phi_u$ state dissociating to the Li(2s) + Li(4f) has a different symmetry than the other $^1\Pi_u$ states. Thus, it can cross other states. The crossing actually takes place, as the $^1\Phi_u$ state is the lowest state in the chemical bonding region among the states correlated to Li(2s) + Li(4l) (l = 1, 2, and 3); however, it is the highest state at the dissociation limit. Thus, the reversal in the order of the energies takes place at some intermediate R between the chemical bonding region and the dissociation

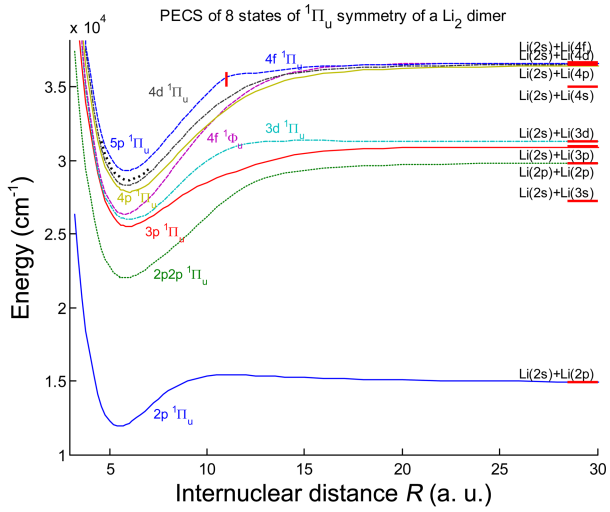

Figure 4. PECs of the eight states of $^1\Pi_u$ symmetry. The highest lying PEC is composed of two different PECs separated by the red vertical bar. The thick dotted line is the PEC of 4f $^1\Pi_u$. It is partially obtained, and its accuracy cannot be guaranteed because it can be found only in a few cases so that no further reduction in error is possible. The PEC is obtained by using the extended JS set augmented with the (3p, 4d, 3f) Kaufmann functions.

limit. Secondly, the seventh $^1\Pi_u$ state, correlated to Li(2s) + Li(4f), is missing in the chemical bonding region in most cases of the calculations due to the root-flipping. The state found most frequently is the 5p $^1\Pi_u$ state, as will be confirmed below [for convenience, a simplified notation such as 2s5p $^1\Pi_u$ or 5p $^1\Pi_u$ is used for the state $^1\Pi_u$ dissociated into Li(2s) + Li(5p)]. In some cases, a missing seventh $^1\Pi_u$ state is found, as shown in Figure 4 by the thick dotted line. It is obtained by using the extended JS set augmented with the (3p, 4d, 3f) Kaufmann functions.

Let us next consider the quantum defect curves (QDCs) $\delta_{2l'nl\lambda}(R)$, defined by[42]

$$U_{2l'nl\lambda}(R) = U^+(R) - \frac{\mathrm{Ry}}{n-\delta_{2l'nl\lambda}(R)]^2}, \qquad (1)$$

where $U_{2l'nl\lambda}(R)$ denotes the PECs for the states belonging to the Rydberg series, either 2snpλ or 2pnpλ, and $U^+(R)$ is the PEC of the appropriate state of a Li_2^+ ion: the PEC of the ground state $X\,^2\Sigma_g^+$ for the 2snpλ Rydberg series and the PEC of the 1 $^2\Pi_u$ state for the 2pnpλ Rydberg series. Ry is the Rydberg constant (109733.026 cm^{-1} for Li_2). $U_{2l'nl\lambda}(R)$ is the PEC shown in Figure 4. The PEC $U^+(R)$ used here is obtained by using the same ECP/CPP method and basis set used in the study reported in Ref. [43]. The active space used is ($4a_g$, $2b_{3u}$, $2b_{2u}$, $4b_{1u}$, $2b_{2g}$, $2b_{3g}$). Twelve state-averaging MRCI calculations are performed. Table 4 show the spectroscopic constants of the Li_2^+ ion calculated from the PECs thus obtained.

Figure 5 shows the QDCs obtained using these PECs with principal quantum numbers n = (2, 2.88, 3, 3, 4, 4, 4, 4) in ascending order of the energies of the states at the dissociation limit. Note that the 2p2p $^1\Pi_u$ state does not belong

Table 4. Spectroscopic constants of the two states of a Li_2^+ ion used in the calculation of the QDCs in the unit of cm^{-1}

	ω_e	B_e	D_e
$X\,^2\Sigma_g^{+43}$	262.60	0.502	10497.53
$X\,^2\Sigma_g^{+52}$	263.1	0.500	10465.3
$1\,^2\Pi_u^{43}$	105.08	0.303	2095.63

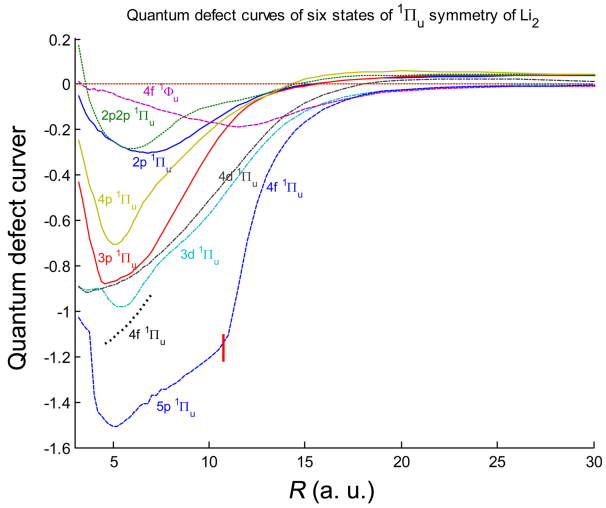

Figure 5. QDCs of eight Rydberg states of $^1\Pi_u$ symmetry converging to the $X\,^2\Sigma_g^+$ state of the Li_2^+ ion. The line style and color follow those of Figure 4.

to the Rydberg series 2snpλ but to the Rydberg series 2pnpλ and thus cannot have n. The value of 2.88 for the 2p2p $^1\Pi_u$ interloper state is conveniently chosen to make its QDC converge to the same limit as the other 2pπ $^1\Pi_u$ states. The value of 2.88 shows that the state lies close to the 3 $^1\Pi_u$ state. The values of the quantum defects at the dissociation limit (R = 88 a_0) are obtained as 0.040, 0.044, 0.0012, –0.0015, 0.045, –0.00096, and -0.0015 for 2p $^1\Pi_u$, 3p $^1\Pi_u$, 3d $^1\Pi_u$, 4f $^1\Phi_u$, 4p $^1\Pi_u$, 4d $^1\Pi_u$, and 4f $^1\Pi_u$, respectively, while the experimental values are 0.041, 0.044, 0.0015, 0.00023, 0.046, 0.0017, and 0.00023. The behaviors of these QDCs at the dissociation limit are the expected behaviors of quantum defects of a Li atom;[44] thus, these are of no interest. However, the behaviors of the QDCs in the chemical bonding region are difficult at first to understand because the QDCs belonging to npπ $^1\Pi_u$ (n = 3-5) are not the same in the range of small R values, which is the Rydberg region where the QDCs belonging to the same Rydberg series are expected to converge into a single curve. Deviation from the expected behavior is due to the perturbation. According to the frame-transformed multichannel quantum defect theory (MQDT), the electron motion is decoupled from the molecular frame at large R values. The electron moves in the average field produced by the electric charge distributions of either the X $^2\Sigma_g^+$ or 1 $^1\Pi_u$ states of the Li_2^+ ion. Figure 6 shows the QDCs obtained by assuming that all eight states are converging to the 1 $^2\Pi_u$ state of the Li_2^+ ion. In other words, they are regarded as a Rydberg series of the type 2pnlλ (λ = 1 and 3).

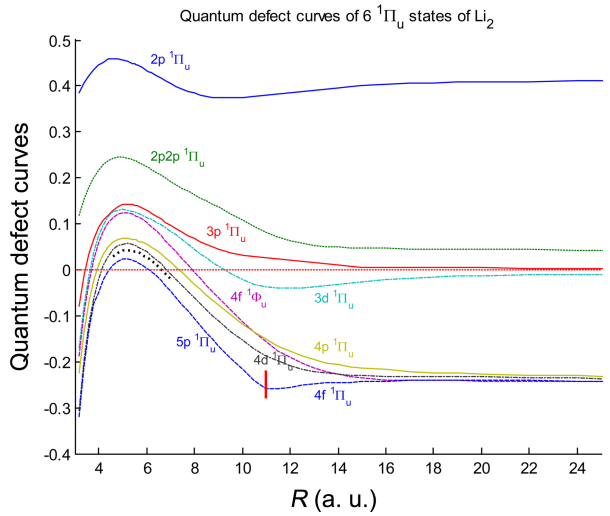

Figure 6. QDCs of eight Rydberg states of $^1\Pi_u$ symmetry converging to the 1 $^2\Pi_u$ state of the Li_2^+ ion. The line style and color follow those of Figure 4.

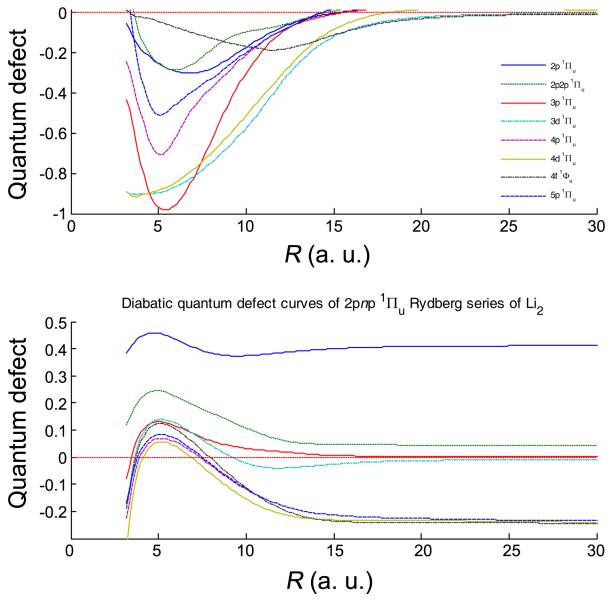

Figure 7. Diabatic QDCs of eight Rydberg states of $^1\Pi_u$ symmetry converging to the X $^2\Sigma_g^+$ and 1 $^2\Pi_u$ states of the Li_2^+ ion. The line style and color shown as a legend in the upper pane are the same as those of Figure 4.

The principal quantum number of all eight states is taken to be the same (2). The similarity of all the QDCs in the chemical bonding region indicates that all the states behave like the same member of the Rydberg series. This means that all are strongly coupled with the interloper and behave in the same way as the interloper. This signifies that all the eight states are strongly perturbed. The extent of the perturbation is large, covering ranges of energy wider than 2000 cm^{-1}.

Perturbation due to an interloper and its effect on the autoionizing Rydberg series has been extensively studied in atomic systems. But, for molecular systems, the study of the effect of an interloper on the Rydberg series is limited only to a few systems. In the case of perturbation to the Rydberg series of a H_2 molecule converging to the ($v^+ = 0$ and $N^+ = 2$) limit because of the interlopers 7pπ $v = 1$ and 5pπ $v = 2$,[45,46] the extent of the perturbation is quite limited (less than 10 cm^{-1}). The seemingly broad range (< 20 cm^{-1}) of perturbation in the observed spectra in the neighborhood of the interlopers is due to the coupling between the two interlopers. Here the extent of the perturbation is larger than 2000 cm^{-1}.

Avoided crossings between 3p $^1\Pi_u$ and 3d $^1\Pi_u$ at R ~4.7 a_0 and 6.6 a_0 also distort the typical patterns expected in the Rydberg series. However, diabatic QDCs for 3p $^1\Pi_u$ and 3d $^1\Pi_u$ can be easily identified. The shape of the QDC for 3d $^1\Pi_u$ is indeed similar to the monotonically increasing shape for 4d $^1\Pi_u$. The region around the minimum of the QDC at ~5.4 a_0 for 3d $^1\Pi_u$ actually corresponds to that for 3p $^1\Pi_u$. In this way, we can construct diabatic QDCs converging to the X $^2\Sigma_g$ state of the Li_2^+ ion as shown in Figure 7. If there were no interlopers, the QDCs of all the members of the 2s*n*pπ Rydberg series would come together into a single curve in the Rydberg region (small R region) and would have positive values. Actually, they go down, reach a minimum at $n = 3$, and then rise again as seen in Figure 7. That is, the minima of the QDCs of the 2s*n*pπ Rydberg series vary as –0.30, –0.98, –0.71, –0.44 as n varies from 2 to 5. The variation of the potential minima reveals that the perturbation is strongest at $n = 3$.

In contrast to the rapid change in the *n*pπ Rydberg series, the 3d and 4d members of the *n*dπ Rydberg series remain almost unchanged though their values in the Rydberg region are extraordinarily large in magnitude. This means that they are strongly perturbed by the interloper, but the perturbation acts almost identically for both the 3d and 4d members. As can be seen in Figure 5, the behaviors of the *n*fπ Rydberg series cannot be characterized with certainty. There are two segments of the QDCs corresponding to the 4fπ member. One segment of the QDC is shown by the thick dotted line at small R values, and the other segment is at $R > 12$ a_0. The

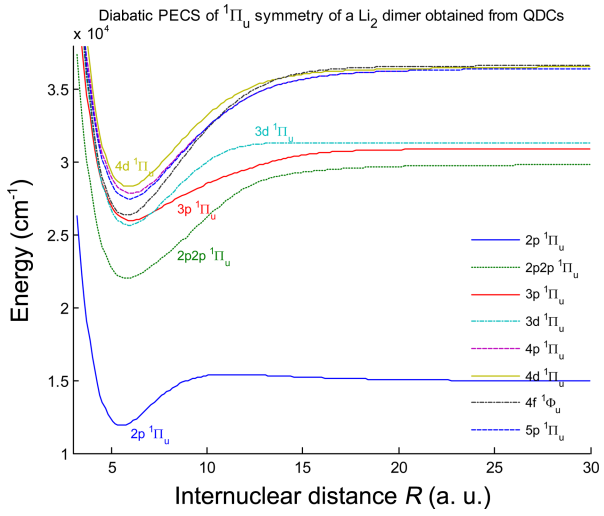

Figure 8. Diabatic PECs of eight states of $^1\Pi_u$ symmetry.

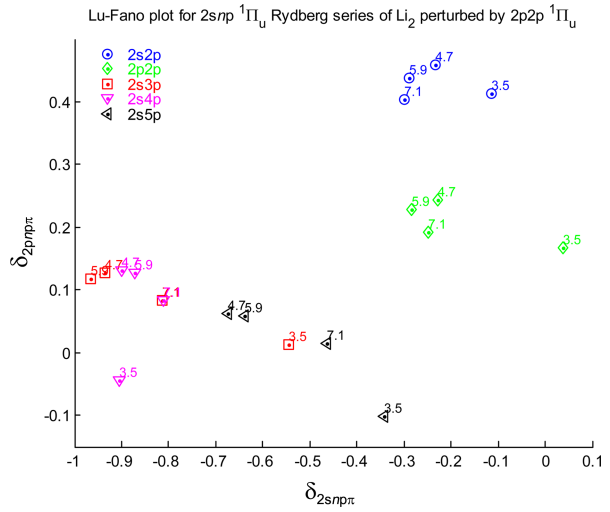

Figure 9. The Lu-Fano plot. The numbers on the markers denote the values of internuclear distance where the quantum defect values are considered.

two segments are not smoothly connected, presumably because of the error due to the numerical instability in the calculations. However, it may be assumed that the 4fπ member behaves similarly to, but lies lower than the QDC of the *n*dπ series. Overall, we have a system of very strong *l*-mixing, including p, d, and f orbitals. This kind of *l*-mixing is theoretically possible but rarely encountered, in contrast to the most common s-d mixing.

Using these QDCs, diabatic PECs can be constructed as shown in Figure 8. Then, with these diabatic PECs, the QDCs converging to the 1 $^2\Pi_u$ state of the Li_2^+ ion can be constructed as shown in Figure 7. Using these QDCs, the Lu-Fano plot[47] can be drawn as shown in Figure 9. The Lu-Fano plot clearly shows the rapid change of the QDCs in the neighborhood of the perturber. Members of the series are separated into two groups: appearing before and after the interloper. Therefore, quantum defects undergo a rapid change around the interloper, with those of the interloper lying in the middle. It may be worthwhile performing MQDT calculations with the diabatic QDCs.[48] Such calculations are beyond the scope of this paper and will be performed in future.

Calculations of the Spectroscopic Constants of the $^1\Pi_u$ States. Table 5 shows the spectroscopic constants for the Π and Φ states calculated using the PECs obtained in the previous section. The spectroscopic constants of the other Π states besides the $^1\Pi_u$ and $^1\Phi_u$ states are also included in the table because they are also calculated as a byproduct in the state-averaged MRCI calculations. The main discussion is focused on the $^1\Pi_u$ and $^1\Phi_u$ states. For 1 $^1\Pi_u$ and 2 $^1\Pi_u$, the agreements between the theoretical and experimental values are very good for R_e, D_e, B_e, and ω_e. However, the errors in T_e can be as large as 70 cm^{-1} for 2 $^1\Pi_u$. The experimental determination of the spectroscopic constants for 3 $^1\Pi_u$ and 4 $^1\Pi_u$ has not been successful.[24] The spectroscopic constants are determined only for each vibrational band by Theiss *et al.*[24] They attributed this failure in determining the spectroscopic constants for all the measured line positions to the homogeneous perturbation from the $^1\Sigma_u$ states. However, Jedrzejewski-Szemek *et al.* reinterpreted Theiss's data and concluded that the eleven vibrational bands observed do not belong to the same D $^1\Pi_u$ state but are a composite of two bands belonging to two different electronic states, 3 $^1\Pi_u$ and 4 $^1\Pi_u$.[37] Table 5 shows the experimental spectroscopic constants of 3 $^1\Pi_u$ and 4 $^1\Pi_u$ obtained using their reinterpretation. The agreement of the spectroscopic values based on the reinterpretation with the values obtained from the PECs of this work is not good.

There is also the assignment problem for 4 $^1\Pi_u$. In Ref. [15], the dissociation product of this state is assigned as (2s+3p), while it has been assigned as (2s+3d) in other studies. This work supports the latter assignment. For 5 $^1\Pi_u$ and 6$^1\Pi_u$, the agreements between the theoretical and experimental values reported in Refs. [35] and [36] are very good. However, for the dissociation product of 6 $^1\Pi_u$, Jedrzejewski-Szemek *et al.* changed their assignment from (2s+4d)[36] to (2s+4p).[15] The assignment was probably changed to group the three newly found states together with D $^1\Pi_u$ and 6 $^1\Pi_u$ into one single Rydberg series. This grouping is based on the values of the quantum defects. The quantum defects of the newly grouped states lie close together around −0.84. They are assigned to the 2s*n*pπ Rydberg series. If the behavior of the QDCs for 2s3dπ and 2s4dπ hold for other members of the 2s*n*dπ series as shown in Figure 5, it may be more natural to assign this Rydberg series as a 2sndπ series. Then, the assignment problem for the D 1Π_u and 6 $^1\Pi_u$ states is resolved.

Another assignment issue is raised in Ref. [15] with regard to the state assigned here as 7 $^1\Pi_u$, correlated to the Li(2s) + Li(4f) limit, or simply as 4f $^1\Pi_u$. This state is assigned as 5p $^1\Pi_u$ by Ross *et al.*[38] mainly because of the value of -5.06 of the effective quantum number of this state. As we can see in Figure 5, it may be acceptable for the quantum defect of 4f $^1\Pi_u$ to be around −1. This unusual value of −5.06 is due to the strong perturbation caused by the interloper 2p2p $^1\Pi_u$. Jedrzejewski-Szemek *et al.* speculated that this state is most likely 4d $^1\Pi_u$.

Results and Discussion

The lithium dimer has drawn an enormous amount of attention from experimentalists and theoreticians. Because of the easy accessibility of excited states by single- and two-photon visible dye lasers, extensive experimental data are available. The lithium dimer is also the smallest bound homonuclear molecule beyond H_2, and accurate quantum chemical calculations are possible. Strangely, all-electron *ab initio* calculations have rarely been used for this molecule; most theoretical calculations are performed using the ECP/CPP method. In this work, calculations using an all-electron *ab initio* method, augmented with the Kaufmann basis functions, were performed. A comparison of the all-electron *ab initio* results with those of ECP/CPP calculations and with the experimental data revealed the deficiency of the all-electron *ab initio* method. The deficiency is related to the

Table 5. Spectroscopic constants of the Π and Φ states of $^7Li_2$

State	Dissociation	Method	R_e (Å)	T_e (cm^{-1})	D_e (cm^{-1})	B_e (cm^{-1})	ω_e (cm^{-1})
1 $^1\Pi_g$	(2s+2p)	This work	4.047	21939.61	1432.799	0.293	89.82
		Exp.[53]	4.058	21988.5	1422.4	0.292	93.35
		Exp.[54]		21998.8	1421.98		92.77
2 $^1\Pi_g$	(2p+2p)	This work	3.191	31781.29	6495.009	0.472	229.36
		Exp.[55]	3.201	31868.4	6455	0.4689	229.26
		Exp.[56]	3.198	31868.02	7679.56	0.46986	229.71
3 $^1\Pi_g$	(2s+3p)	This work	3.172	35276.75	4117.149	0.478	229.29
		Exp.[57]		35360.761		0.4745	228.9824
4 $^1\Pi_g$	(2s+3d)	This work	3.156	37169.02	2582.6	0.508	304.92
		Exp.[57]		37257.700		0.4794	237.3867
1 $^1\Pi_u$	(2s+2p)	This work	2.930	20392.66	2979.749	0.551	273.6
		Exp.[29]		20436	2984.42		270.69
2 $^1\Pi_u$	(2p+2p)	This work	3.071	30478.92	7797.379	0.508	241.58
		Exp.[33]	3.074	30548.99	7775.9	0.50845	239.103
		Exp.[32]	3.080	30550.862		0.50657	238.165
		Exp.[34]	3.081	30550.52	7773.7		
3 $^1\Pi_u$	(2s+3p)	This work	3.156	33968.61	5425.289	0.482	236.53
		Exp.[24,37]	3.235	34120.5		0.459	197.7
4 $^1\Pi_u$	(2s+3d)	This work	3.191	34452.12	5299.499	0.472	202.14
		Exp.[24,37]	3.487	34529.7		0.395	208.6
		Exp.[15]		34605.7	4942		
1 $^1\Phi_u$	(2s+4f)	This work	3.068	34817.63	10120.44	0.511	267.69
5 $^1\Pi_u$	(2s+4p)	This work	3.198	36324.65	8767.269	0.47	230.37
		Exp.[35]	3.2033	36390.97	8595.2	0.468321	232.035
		Theory[39]		36512		0.4736	232.2
6 $^1\Pi_u$	(2s+4d)	This work	3.120	36785.56	8313.159	0.494	251.39
		Exp.[36]	3.164	36863.25	8276.7	0.480072	253.567
		Theory[39]	3.107	36914		0.4976	256.2
7 $^1\Pi_u$	(2s+4f)	This work	3.138	37135.15	7956.69	0.488	247.30
		Exp.[38]		37259		0.511	262.45
8 $^1\Pi_u$	(2s+5p)	This work	3.110	37775.45	7323.27	0.493	267.73
2 $^3\Pi_g$	(2p+2p)	This work	3.855	29762.83	8513.56	0.323	189.47
		Exp.[58]	3.816	29840.5	8484		189.1
		Exp.[59]	3.846	29844.69	8479.621	0.3255	188.659
		Exp.[9]	3.842	29844.24		0.326	188.644
		Theory[9]	3.922	29742			
3 $^3\Pi_g$	(2s+3p)	This work	3.122	33284.17	3327.089	0.493	253.79
		Exp.[9]	3.047	33638.99		0.518	253.356
		Theory[9]	3.175	33456			
4 $^3\Pi_g$	(2s+3d)	This work	3.105	36424.53	12314.11	0.499	259.22
1 $^3\Pi_u$	(2s+2p)	This work	2.577	11058.3	12314.11	0.724	347.31
		Exp.[60]	2.590	11236	12178		345.6
2 $^3\Pi_u$	(2p+2p)	This work	2.966	29531.37	8745.02	0.546	282.67
3 $^3\Pi_u$	(2s+3p)	This work	3.991	33610.41	5783.48	0.302	222.55
4 $^3\Pi_u$	(2s+3d)	This work	3.063	34716.68	5034.939	0.512	245.01

mere 51.9% attainment of electron correlation for the ground state by the MRCI method. The percent attainment of electron correlation for the first excited state is slightly better than that for the ground state, indicating that the agreement of theoretical values with the observed ones cannot be improved by increasing the size of the Rydberg basis set.

We applied the Kaufmann basis method to the ECP/CPP method in order to obtain accurate, convergent PECs for the $^1\Pi_u$ states correlated to Li(2p) + Li(2p) and Li(2s) + Li(n = 2, 3, 4). Among the two states $^1\Pi_u$ and $^1\Phi_u$ correlated to Li(2s) + Li(4f), the former is obtained only for limited cases and for a limited range of internuclear distances R. The PEC of the latter is the lowest energy state in the chemical bonding region among the states correlated to Li(2s) + Li(n = 4),

although it is the highest energy state at the dissociation limit. Because of this reversal in the order of energies, it crosses all the other states correlated to Li(2s) + Li(n = 4). Using the PECs, quantum defect curves (QDCs) were calculated both for the X $^2\Sigma_g$ and 1 $^2\Pi_u$ states of the Li_2^+ ion in order to examine the series-series interaction of the 2snpπ and 2pnpπ Rydberg series. The QDCs obtained by assuming the convergence of all eight states to the 1 $^2\Pi_u$ state of the Li_2^+ ion with the same principal quantum number 2 showed similarities in the chemical bonding region, indicating that all the states behave just like the same member of the Rydberg series. This means that all are strongly coupled with the interloper and behave in the same way as the interloper. The extent of the perturbation is large, covering ranges of energy larger than 2000 cm^{-1}.

The QDCs were also used to resolve assignment problems in the literature. Using our results, the assignment problem existing for the $^1\Pi_u$ states in the literature is re-examined. Jedrzejewski-Szemek *et al.*[15] assigned the dissociation product of this state as (2s+3p), while others assigned it as (2s+3d). Jedrzejewski-Szemek *et al.* changed the assignment of the dissociation product of 6 $^1\Pi_u$ from the original (2s+4d) to (2s+4p), probably to group the three newly found states into one single Rydberg series. This grouping is based on the values of the quantum defects. The newly grouped states have very close values of quantum defects around −0.84. They are assigned to the 2snpπ Rydberg series. Actually, it may be more natural to assign this Rydberg series as a 2sndπ series, as discussed in the previous section. With this reassignment of their Rydberg series from 2snpπ to 2sndπ, their assignments for the D $^1\Pi_u$ and 6 $^1\Pi_u$ states are now restored to the previous assignments (2s+3d) and (2s+4d), respectively. Another assignment issue raised in Ref. [15] is the state assigned here as the 7 $^1\Pi_u$ state, correlated to the Li(2s) + Li(4f) limit, or simply as 4f $^1\Pi_u$. This state is assigned as 5p $^1\Pi_u$ by Ross *et al.*[38] mainly because of the value of −5.06 of the effective quantum number of this state. As seen in Figure 5, it may be acceptable for the quantum defect of 4f $^1\Pi_u$ to be around −1. This unusual value of −5.06 is due to the strong perturbation caused by the interloper 2p2p $^1\Pi_u$. Jedrzejewski-Szemek *et al.* speculated that this state is most likely 4d $^1\Pi_u$, but their reasoning is poor.

Acknowledgments. This study was supported by the Basic Science Research Program through the National Research Foundation of Korea (NRF) funded by the Ministry of Education, Science and Technology (2011-0024808).

References

1. Werner, H.-J. *Adv. Chem. Phys.* **1987**, *69*, 1.
2. Lefebvre-Brion, H.; Moser, C. M. *J. Chem. Phys.* **1965**, *43*, 1394.
3. Kaufmann, K.; Baumeister, W.; Jungen, M. *J. Phys. B* **1989**, *22*, 2223.
4. Lee, C.-W.; Gim, Y. *J. Phys. B* **2013**, *46*, 215001.
5. Ketterle, W.; Messmer, H. P.; Walther, H. *Phys. Rev. A* **1989**, *40*, 7434.
6. Ketterle, W. *J. Chem. Phys.* **1990**, *93*, 6935.
7. van Hemert, M. C.; Peyerimhoff, S. D. *J. Chem. Phys.* **1991**, *94*, 4369.
8. Olson, M. L.; Konowalow, D. D. *Chem. Phys. Lett.* **1976**, *39*, 281.
9. Yiannopoulou, A.; Urbanski, K.; Antonova, S.; Lyyra, A. M.; Li, L.; An, T.; Whang, T. J.; Ji, B.; Wang, X. T.; Stwalley, W. C.; Leininger, T.; Jeung, G. H. *J. Chem. Phys.* **1995**, *103*, 5898.
10. Song, M.; Yi, P.; Dai, X.; Liu, Y.; Li, L.; Jeung, G. H. *J. Mol. Spectrosc.* **2002**, *215*, 251.
11. Qi, P.; Lazarov, G.; Marjatta Lyyra, A.; Jeung, G.-H. *J. Mol. Spectrosc.* **2008**, *247*, 184.
12. Schmidt-Mink, I.; Müller, W.; Meyer, W. *Chemical Physics* **1985**, *92*, 263.
13. Jasik, P.; Sienkiewicz, J. E. *Chemical Physics* **2006**, *323*, 563.
14. Fuentealba, P.; Preuss, H.; Stoll, H.; Von Szentpály, L. *Chem. Phys. Lett.* **1982**, *89*, 418.
15. Grochola, A.; Kowalczyk, P.; Jastrzebski, W. *J. Phys. B* **2010**, *43*, 155102.
16. Werner, H.-J.; Knowles, P. J.; Knizia, G.; Manby, F. R.; Schutz, M.; others; MOLPRO, version 2012.1, www.molpro.net.
17. Dunning, T. H. *J. Chem. Phys.* **1989**, *90*, 1007.
18. Chun-Woo, L.; Yeongrok, G. *Journal of Physics B: Atomic, Molecular and Optical Physics* **2013**, *46*, 215001.
19. Roos, B. O. *Int. J. Quantum Chem.* **1980**, *18*, 175.
20. Rees, A. L. G. *Proc. Phys. Soc.* **1947**, *59*, 998.
21. Pashov, A.; Jastrz?bski, W.; Kowalczyk, P. *Comput. Phys. Commun.* **2000**, *128*, 622.
22. Coxon, J. A.; Melville, T. C. *J. Mol. Spectrosc.* **2006**, *235*, 235.
23. Eisel, D.; Demtröder, W.; Müller, W.; Botschwina, P. *Chemical Physics* **1983**, *80*, 329.
24. Theiss, W.; Müschenborn, H. J.; Demtröder, W. *Chem. Phys. Lett.* **1990**, *174*, 126.
25. Weyh, T.; Lokai, S.; Demtröder, W. *Chem. Phys. Lett.* **1996**, *257*, 453.
26. Schwarz, M.; Duchowicz, R.; Demtroder, W.; Jungen, C. *J. Chem. Phys.* **1988**, *89*, 5460.
27. Rai, S. B.; Hemmerling, B.; Demtröder, W. *Chemical Physics* **1985**, *97*, 127.
28. Bouloufa, N.; Cacciani, P.; Vetter, R.; Yiannopoulou, A. *J. Chem. Phys.* **1999**, *111*, 1926.
29. Bouloufa, N.; Cacciani, P.; Vetter, R.; Yiannopoulou, A.; Martin, F.; Ross, A. J. *J. Chem. Phys.* **2001**, *114*, 8445.
30. Bouloufa, N.; Cacciani, P.; Kokoouline, V.; Masnou-Seeuws, F.; Vetter, R.; Li, L. *Phys. Rev. A* **2001**, *63*, 042507.
31. Cacciani, P.; Kokoouline, V.; Bouloufa, N.; Masnou-Seeuws, F.; Vetter, R. *Phys. Rev. A* **2003**, *68*, 042506.
32. Kasahara, S.; Kowalczyk, P.; Kabir, M. H.; Baba, M.; Katô, H. *J. Chem. Phys.* **2000**, *113*, 6227.
33. Ishikawa, K.; Kubo, S.; Katô, H. *J. Chem. Phys.* **1991**, *95*, 8803.
34. Kubkowska, M. K.; Grochola, A.; Jastrzebski, W.; Kowalczyk, P. *Chemical Physics* **2007**, *333*, 214.
35. Jędrzejewski-Szmek, Z.; Grochola, A.; Jastrzebski, W.; Kowalczyk, P. *Chem. Phys. Lett.* **2007**, *444*, 229.
36. Grochola, A.; Jastrzebski, W.; Kowalczyk, P. *Molecular Physics* **2008**, *106*, 1375.
37. JęDrzejewski-Szmek, Z.; Grochola, A.; Jastrzębski, W.; Kowalczyk, P. *Optica Applicata* **2010**, *40*, 577.
38. Ross, A. J.; Martin, F.; Adohi-Krou, A.; Jungen, C. *J. Mol. Spectrosc.* **2004**, *227*, 158.
39. Spies, N., Universitaet Kaiserslautern, 1990.
40. Jasik, P.; Sienkiewicz, J. E. In *41st EGAS*; Kwela, J., Wasowicz, T. J., Eds.; Gdansk, Poland, 2009.
41. Gadéa, F. X.; Leininger, T. *Theor. Chem. Acc.* **2006**, *116*, 566.
42. Mulliken, R. S. *Acc. Chem. Res.* **1976**, *9*, 7.
43. Jasik, P.; Wilczyński, J.; Sienkiewicz, J. E. *The European Physical Journal Special Topics* **2007**, *144*, 85.
44. Gallagher, T. F. *Rydberg Atoms*; Cambridge University Press: Cambridge; New York, 1994.
45. Jungen, C.; Dill, D. *J. Chem. Phys.* **1980**, *73*, 3338.

46. Lee, C. W. *Bull. Korean Chem. Soc.* **2012**, *33*, 2657.
47. Fano, U.; Rau, A. R. P. *Atomic Collisions and Spectra*; Academic: Orlando, USA, 1986.
48. Atabek, O.; Dill, D.; Jungen, C. *Phys. Rev. Lett.* **1974**, *33*, 123.
49. Froese Fischer, C.; Brage, T.; Jönsson, P. *Computational Atomic Structure : An MCHF Approach*; Institute of Physics Pub.: Bristol; Philadelphia, PA, 1997.
50. Accad, Y.; Pekeris, C. L.; Schiff, B. *Phys. Rev. A* **1971**, *4*, 516.
51. Carlsson, J.; Jönsson, P.; Froese Fischer, C. *Phys. Rev. A* **1992**, *46*, 2420.
52. Roche, A. L.; Jungen, C. *J. Chem. Phys.* **1993**, *98*, 3637.
53. Miller, D. A.; Gold, L. P.; Tripodi, P. D.; Bernheim, R. A. *J. Chem. Phys.* **1990**, *92*, 5822.
54. Linton, C.; Martin, F.; Bacis, R.; Vergès, J. *J. Mol. Spectrosc.* **1990**, *142*, 340.
55. Bernheim, R. A.; Gold, L. P.; Kelly, P. B.; Tipton, T.; Veirs, D. K. *J. Chem. Phys.* **1981**, *74*, 2749.
56. Bernheim, R. A.; Gold, L. P.; Kelly, P. B.; Kittrell, C.; Veirs, D. K. *Phys. Rev. Lett.* **1979**, *43*, 123.
57. Bernheim, R. A.; Gold, L. P.; Tipton, T. *J. Chem. Phys.* **1983**, *78*, 3635.
58. Xie, X.; Field, R. W. *J. Mol. Spectrosc.* **1986**, *117*, 228.
59. Li, D.; Xie, F.; Li, L.; Lazoudis, A.; Lyyra, A. M. *J. Mol. Spectrosc.* **2007**, *246*, 180.
60. Engelke, F.; Hage, H. *Chem. Phys. Lett.* **1983**, *103*, 98.
61. Pashov, A.; Jastrzebski, W.; Kowalczyk, P. *J. Chem. Phys.* **2000**, *113*, 6624.
62. Ivanov, V. S.; Sovkov, V. B.; Li, L.; Lyyra, A. M.; Lazarov, G.; Huennekens, J. *J. Mol. Spectrosc.* **1999**, *194*, 147.